The Finite-Element Modeling of Three-Dimensional Electromagnetic Fields Using Edge and Nodal Elements

Gerrit Mur

Abstract— **An efficient and accurate finite-element method is presented for computing transient as well as time-harmonic electromagnetic fields in three-dimensional configurations containing arbitrarily inhomogeneous media that may be anisotropic. To obtain accurate results with an optimum computational efficiency, both consistently linear edge and consistently linear nodal elements are used for approximating the spatial distribution of the field. Compared with earlier work, our formulation is generalized by adding a method for explicitly modeling the normal continuity along interfaces that are free of surface charge. In addition to this the conditions for efficiently solving time-harmonic problems using a code designed for solving transient problems are discussed. Finally a general and simple method for implementing arbitrary inhomogeneous absorbing boundary conditions for modeling arbitrary incident fields is introduced.**

I. Introduction

In view of its flexibility the finite-element method is very suitable for computing electromagnetic fields in inhomogeneous media and/or complicated configurations. When computing electromagnetic fields in inhomogeneous media in terms of the electric or magnetic field strength, it is necessary to use a computational technique that accounts for the continuity of the tangential components of the fields across interfaces between different media and that allows for a jump in the normal components of these field strengths. Some authors [1], [2] solve this difficulty by subdividing the problem space into a number of homogeneous subdomains. The boundary conditions at interfaces are then imposed separately. This technique, however, may yield inaccurate results because of the conflicting continuity conditions at nodes where the vector normal to the interfaces is not unique. Alternatively, this difficulty can be solved by using potentials [3], [4]. Approaches of this type have a number of disadvantages, the most important of them being that a numerical differentiation is required for computing the electric or magnetic field strength from these potentials. This causes a large loss of accuracy and, consequently, a poor convergence of the resulting accuracy as a function of the mesh size.

The difficulty of modeling the conditions along interfaces can be solved at the element level by using edge elements [5]. Edge elements have been designed to account for the continuity of the tangential components of the fields across interfaces. They allow for a jump in the normal components of the field strengths such that the continuity conditions applying to the normal flux can be satisfied. Additional advantages of edge-based elements are that they do not generate conflicting conditions at the nodes where the vector normal to an interface or outer boundary is not unique and that they automatically provide a natural representation of the tangential field strengths along the outer boundary for all possible orientations of this boundary. Computationally, edge elements have the disadvantage of being much more expensive than the commonly employed nodal elements that make all field components continuous and that represent the field accurately only in media where the constitutive coefficients are continuous functions of the spatial coordinates. In [6] it was shown for time-harmonic problems that using a combination of edge elements and nodal elements for the expansion of the electric or magnetic field strength yields optimum computational results. By adding the divergence condition [7], [8], the latter formulation was further improved, both with regard to its computational efficiency (storage and time) and its accuracy. In [9] it was shown that the combination of edge and nodal elements mentioned above can also be used in a mixed formulation of the three-dimensional time-domain Maxwell equations. In the latter paper, an explicit method was used for the integration of the system of coupled differential equations along the time axis. In [10] the explicit mixed time-domain formulation was replaced by an implicit irreducible one in terms of the electric field strength only. The irreducible formulation was chosen both to make it easier to implement implicit methods for carrying out the integration along the time axis and to reduce the storage requirements. Experimental numerical results confirming the theoretical convergence estimates were given. In the present paper we shall describe an improved and augmented version of our formulation and give some numerical results for a simple but realistic configuration with inhomogeneous lossy media.

Elements that exactly preserve tangential continuity without imposing conditions on the normal components have been proposed before [11]. The disadvantage of the elements discussed in [11] is that they are of mixed order, and for this

Manuscript received September 8, 1992; revised January 15, 1993. This work was supported by the Stichting Fund for Science, Technology and Research (a companion organization to the Schlumberger Foundation in the U.S.), Schlumberger-Doll Research, Ridgefield, CT, Etudes et Productions Schlumberger, Clamart, France, and Schlumberger Cambridge Research Limited, Cambridge, England.

The author is with the Laboratory of Electromagnetic Research, Faculty of Electrical Engineering, Delft University of Technology, P.O. Box 5031, 2600 GA Delft, The Netherlands.

IEEE Log Number 9211260.

reason they yield relatively poor convergence properties [5], [12]; i.e., the accuracy obtained improves only slowly with decreasing mesh size. Linear mixed elements, for instance, are constants along their generating edges, whereas our edge elements are consistently linear; i.e., all components of the vectorial expansion functions are linear functions of all three spatial coordinates.

II. The Choice of the Expansion Functions

For topological reasons, the geometrical domain, $\mathcal{D}$, in which the finite-element method is applied is subdivided into a number of adjoining tetrahedra (simplices in $\mathbb{R}^3$). This subdivision can be done either exactly, when $\mathcal{D}$ is a polyhedron, or approximately if $\mathcal{D}$ has a more general shape. In each tetrahedron $\mathcal{T}$ the set of local nodal expansion functions $\{\boldsymbol{W}_{i,j}^{(\mathrm{C})}(\boldsymbol{x})\}$ is given by $\boldsymbol{W}_{i,j}^{(\mathrm{C})}(\boldsymbol{x}) = \phi_i(\boldsymbol{x})\boldsymbol{i}_j$ $(i = 0,\cdots,3,\ j = 1,2,3)$, where $\boldsymbol{i}_j$ are the base vectors with respect to the (background) Cartesian reference frame and where $\phi_i(\boldsymbol{x})$ are the barycentric coordinates. The set of local edge expansion functions $\{\boldsymbol{W}_{i,j}^{(\mathrm{E})}(\boldsymbol{x})\}$ is given by $\boldsymbol{W}_{i,j}^{(\mathrm{E})}(\boldsymbol{x}) = a_{i,j}\phi_i(\boldsymbol{x})\nabla\phi_j(\boldsymbol{x})$, $(i,j = 0,\cdots,3,\ i \neq j)$, where $a_{i,j} = |\boldsymbol{x}_i - \boldsymbol{x}_j|$ denotes the length of the edge joining the vertices $\boldsymbol{x}_i$ and $\boldsymbol{x}_j$. When $\boldsymbol{x} \in \mathcal{T}$, the electric field strength $\boldsymbol{E}(\boldsymbol{x},t)$ is expanded as

$$\boldsymbol{E}(\boldsymbol{x},t) = \sum_{i=0}^{3}\sum_{j} e_{i,j}(t)\boldsymbol{W}_{i,j}^{(\mathrm{C,E})}(\boldsymbol{x}), \tag{1}$$

where $\{e_{i,j}(t)\}$ denotes the local set of unknown time-dependent expansion coefficients. The expansion functions are, in each tetrahedron, taken from the set $\{\boldsymbol{W}_{i,j}^{(\mathrm{C,E})}(\boldsymbol{x})\} = \{\boldsymbol{W}_{i,j}^{(\mathrm{C})}(\boldsymbol{x}), \boldsymbol{W}_{i,j}^{(\mathrm{E})}(\boldsymbol{x})\}$ since, depending on the local degree of inhomogeneity [6], edge elements will be used along interfaces between different media, and nodal elements will be used in homogeneous subdomains.

III. The System of Differential Equations

Eliminating the magnetic field strength, $\boldsymbol{H}$, from Maxwell's equations, we obtain

$$\begin{aligned}\partial_t^2\boldsymbol{\epsilon}\cdot\boldsymbol{E} + \partial_t\boldsymbol{\sigma}\cdot\boldsymbol{E} + \nabla\times(\boldsymbol{\mu}^{-1}\cdot\nabla\times\boldsymbol{E}) = \\ -\partial_t\boldsymbol{J}^{\mathrm{ext}} - \nabla\times(\boldsymbol{\mu}^{-1}\cdot\boldsymbol{K}^{\mathrm{ext}}),\end{aligned} \tag{2}$$

where $\boldsymbol{J}^{\mathrm{ext}}$ and $\boldsymbol{K}^{\mathrm{ext}}$ denote external sources of electrical and magnetic current, and where $\boldsymbol{\epsilon}$, $\boldsymbol{\sigma}$, and $\boldsymbol{\mu}$ denote the permittivity, the conductivity, and the permeability tensor, respectively. After substituting the expansion (1) for the electric field strength into (2), a system of differential equations in the expansion coefficients is obtained by applying the method of weighted residuals. The set of weighting functions $\{\boldsymbol{W}_{p,q}^{(\mathrm{C,E})}(\boldsymbol{x})\}$ that is used is the same as the set of expansion functions. Using an integration by parts and adding the resulting equations over all tetrahedra, we obtain a system of coupled ordinary differential equations for $\{e_{i,j}\}$ that can be written as

$$\begin{aligned}&\sum_{i,j}\partial_t^2 e_{i,j}\int_{\mathcal{D}}\boldsymbol{W}_{p,q}\cdot\boldsymbol{\epsilon}\cdot\boldsymbol{W}_{i,j}\mathrm{d}V \\ &+\sum_{i,j}\partial_t e_{i,j}\int_{\mathcal{D}}\boldsymbol{W}_{p,q}\cdot\boldsymbol{\sigma}\cdot\boldsymbol{W}_{i,j}\mathrm{d}V \\ &+\sum_{i,j}e_{i,j}\int_{\mathcal{D}}(\nabla\times\boldsymbol{W}_{p,q})\cdot\boldsymbol{\mu}^{-1}\cdot(\nabla\times\boldsymbol{W}_{i,j})\mathrm{d}V = \\ &\quad\partial_t\int_{\partial\mathcal{D}}\boldsymbol{W}_{p,q}\cdot(\boldsymbol{n}\times\boldsymbol{H})\mathrm{d}A \\ &\quad-\partial_t\int_{\mathcal{D}}\boldsymbol{W}_{p,q}\cdot\boldsymbol{J}^{\mathrm{ext}}\mathrm{d}V \\ &\quad-\int_{\mathcal{D}}(\nabla\times\boldsymbol{W}_{p,q})\cdot\boldsymbol{\mu}^{-1}\cdot\boldsymbol{K}^{\mathrm{ext}}\mathrm{d}V\ \forall p,q,\end{aligned} \tag{3}$$

where $\partial\mathcal{D}$ denotes the outer boundary of the domain of computation $\mathcal{D}$ and $\boldsymbol{n}$ the unit vector along the outward normal to $\partial\mathcal{D}$. For deriving (3) we have used the continuity of the tangential components of the magnetic field strength over all internal interfaces.

Assuming the medium in each tetrahedron to be homogeneous and assuming no initial charges, it follows from Maxwell's equations that the electric flux density, $\boldsymbol{D} = \boldsymbol{\epsilon}\cdot\boldsymbol{E}$, should be free of divergence in each tetrahedron. This condition is not automatically enforced by (3). To impose freedom of divergence, the system of differential equations (3) is modified by adding the conditions

$$\sum_{i,j}e_{i,j}\int_{\mathcal{T}}(\nabla\cdot\boldsymbol{W}_{p,q})|\boldsymbol{\epsilon}\cdot\boldsymbol{\mu}|^{-1}\nabla\cdot(\boldsymbol{\epsilon}\cdot\boldsymbol{W}_{i,j})\mathrm{d}V = 0\ \forall p,q \tag{4}$$

to it for all tetrahedra $\mathcal{T}$. Observe that the validity of (4) follows from the divergence condition and that it has the same dimension as the terms in (3). As regards the validity of (4) we further note that, since our elements are not free of divergence themselves, it is not enforced by either the edge elements or the Cartesian elements used. Because of this the divergence condition must be made a part of the formulation of the problem. In case of anisotropy, the norm in (4) has to be taken such that it reduces to $\varepsilon\mu$ for isotropic media.

When we have an interface between two different lossless media carrying no initial surface charges it follows from Maxwell's equations that the normal component of the electric flux density should be continuous across this interface. This condition is not enforced explicitly by (3); it can be imposed by adding the conditions

$$\int_{\partial\mathcal{T}}\boldsymbol{n}\cdot(\boldsymbol{D}^{+}-\boldsymbol{D}^{-})\mathrm{d}A = 0 \tag{5}$$

to it for all triangles $\partial\mathcal{T}$ along this part of the interface. In (5) $\boldsymbol{n}$ denotes the normal to $\partial\mathcal{T}$ and $\boldsymbol{D}^{+}$ and $\boldsymbol{D}^{-}$ denote the electric flux densities at both sides of this triangular interface between two tetrahedra. The use of (5) will cause the connectivity of the problem to increase, and for this reason some additional nonzero elements will be added to the system matrices. In practical cases, when the number of tetrahedra connected to interfaces is small compared with the number of tetrahedra covering the "homogeneous" subdomains, this increase is of the order of a few percent; in extremely inhomogeneous configurations it will be higher depending on the degree of inhomogeneity. The element matrices implied in (5) are asymmetric. In order to avoid a disruption of the symmetry of the system matrices derived from (3), these element matrices are symmetrized by multiplying them by their transpose before adding them to the relevant system matrix. Using the above procedures, the divergence condition is imposed in a weighted sense. A numerical solution that is obtained using (4) and (5) will be free of divergence in the numerical sense, i.e. the divergence condition is satisfied to the same degree of accuracy as (2) is. Because of this our method does not suffer from difficulties like "spurious modes".

The system of coupled differential equations can, in matrix form, be written as

$$\boldsymbol{M}_{\varepsilon}\mathrm{d}_t^2\boldsymbol{e}(t) + \boldsymbol{M}_{\sigma}\mathrm{d}_t\boldsymbol{e}(t) + \boldsymbol{M}_{\mu}\boldsymbol{e}(t) = \boldsymbol{q}(t). \tag{6}$$

Together with the appropriate initial and boundary conditions (6) constitutes a system of coupled ordinary diffential equations from which the evolution in time of the expansion coefficients can be obtained. When the problem to be solved contains Dirichlet boundary conditions, some of the elements of the vector $\boldsymbol{e}(t)$ will have prescribed, generally time-dependent, values. Those elements should be eliminated from the vector of unknowns $\boldsymbol{e}(t)$, and (6) has to be rewritten such that their contribution is added to the relevant part of right-hand side vector $\boldsymbol{q}(t)$.

IV. The Integration of the System of Differential Equations

For the integration of the system of coupled differential equations (6) along the time axis the most obvious chioces are single- and two-step time marching schemes [13], [14]. We have used both methods with a number of different weighting functions in time. As regards computational efficiency, two-step methods have proved to be slightly more efficient for solving our type of problems than single-step methods.

Using an incomplete LU decomposition [15] of the system matrix for preconditioning, the iterative (conjugate-gradient) solution of the system of linear algebraic equations that has to be determined for each time-step has proved to be an extremely fast method, requiring only a few (usually two to 20) iteration steps for each time step.

Time-Harmonic Problems

Complex valued time-harmonic fields can be computed in the time domain by, for instance, using a pulse excitation and using Fourier transformations to select the desired temporal frequencies. This method is expensive in terms of time and storage requirements but it has the advantage of yielding results for a range of frequencies rather than for a single frequency.

Alternatively, one can switch on the time-harmonic sources at $t = 0$, say, and continue the time stepping until steady state is achieved. The duration of this process can be estimated as follows. After starting the time stepping process the solution will consist of the exact time-harmonic solution together with an error that has to be eliminated by letting it decay in time. This error term will contain terms in a wide temporal frequency range. Assuming, for simplicity, homogeneous media, high-frequency terms will decay with the well-known time constant ε/σ. It is easily shown that low-frequency terms will decay with a time constant $\mu\sigma L_{\mathcal{D}}^2$, where $L_{\mathcal{D}}$ is a length typical for the outer dimensions of the domain of computation $\mathcal{D}$. Error terms having intermediate frequencies will decay with a speed that is inversely proportional to the Q factor of the configuration studied. Numerical experience has shown that the largest of these time constants, usually the one related to low-frequency errors, is often such that an excessively large number of time steps is required to obtain steady state within a sufficient degree of accuracy.

In order to speed up the computations we modified the above computational procedure by not switching on the time-harmonic sources abruptly at $t = 0$, but by introducing a transient period $0 \le t \le t_{\mathrm{tr}}$. During this period the right-hand side vector $\boldsymbol{q}(t)$ representing the time-harmonic excitation, is multiplied by a continuous function $f_{\mathrm{tr}}(t)$ that generates a smooth transient from zero to steady state. For f_{tr} we use the function

$$\begin{aligned} f_{\mathrm{tr}} &= 0, \qquad -\infty < t < 0,\\ &= (2 - \sin((t/t_{\mathrm{tr}})\pi/2))\sin((t/t_{\mathrm{tr}})\pi/2),\\ &\qquad 0 \le t \le t_{\mathrm{tr}},\\ &= 1, \qquad t_{\mathrm{tr}} < t < \infty. \end{aligned} \tag{7}$$

Using f_{tr} we obtain, at $t \ge t_{\mathrm{tr}}$, an approximation of the time-harmonic solution with a relatively small error term, and steady state is achieved much faster. In most cases a value of t_{tr} in the range $5T \le t_{\mathrm{tr}} \le 10T$, where T denotes the period in time of the time-harmonic sources, turns out to yield an optimum computational efficiency. Obviously the optimum choice for t_{tr} depends both on the problem at hand and on the accuracy requirements. In general it can be said that t_{tr} should preferably be chosen such that the solution at $t = t_{\mathrm{tr}}$ is already accurate enough to be used as a steady-state solution and that no subsequent time stepping is required to obtain steady state.

V. Inhomogeneous Absorbing Boundary Conditions

Absorbing boundary conditions are used on (parts of) the outer surface of the domain of computation for modeling the unbounded surrounding by absorbing the scattered field that is generated in the domain of computation. In the case where an external field is incident upon the domain of computation, it is necessary to distinguish the scattered field from the incident field. This can be done by introducing an additional mathematical boundary close to the absorbing boundaries [16]. In a finite-element program this is rather difficult to implement and therefore we have adopted another simple and general approach to include the incident field in the absorbing boundary condition.

Suppose we have an arbitrary absorbing boundary condition that can be written in operator form as

$$A(\boldsymbol{E}^{\text{scat}}) = 0. \tag{8}$$

Assuming the operator A to be linear, we add the trivial identity $A(\boldsymbol{E}^{\text{inc}}) = A(\boldsymbol{E}^{\text{inc}})$, where $\boldsymbol{E}^{\text{inc}}$ denotes an arbitrary incident field distribution, to (8) to obtain

$$A(\boldsymbol{E}) = A(\boldsymbol{E}^{\text{inc}}). \tag{9}$$

Now (9) constitutes an inhomogeneous absorbing boundary condition for each incident wave and for each linear homogeneous absorbing boundary condition A. Note that this method of taking the incident field into account does not require the construction of an artificial mathematical boundary; it requires only the generation of the right-hand side of (9). This right-hand side is easily taken into account in (3) and generates a contribution to the right-hand side vector $\boldsymbol{q}(t)$ of (6).

VI. Numerical Results

In [10] we have studied the convergence properties of our method by applying it to a problem for which the exact analytical solution is known. It was shown that the RMS error in the solution is approximately $\mathrm{O}((h/\lambda)^2)$, where h denotes the maximum diameter of a tetrahedron and where λ denotes the wavelength of the incident field.

In the present paper we consider the scattering of a time-harmonic plane wave by an inhomogeneous isotropic cubic scatterer. The scatterer consists of an inner cube covering the region $\mathcal{D}_1$ { -0.075 $\leq x_1 \leq$ 0.075 m, -0.075 $\leq x_2 \leq$ 0.075 m, -0.075 $\leq x_3 \leq$ 0.075 m}, with medium properties $\{\varepsilon_1 = 70\varepsilon_0$ F/m, $\sigma_1 = 0.68$ S/m, $\mu_1 = \mu_0$ H/m}. The inner cube is embedded in a second cube covering the region $\mathcal{D}_2$ { -0.15 $\leq x_1 \leq$ 0.15 m, -0.15 $\leq x_2 \leq$ 0.15 m, -0.15 $\leq x_3 \leq$ 0.15 m}, with medium properties $\{\varepsilon_2 = 7.5\varepsilon_0$ F/m, $\sigma_2 = 0.05$ S/m, $\mu_2 = \mu_0$ H/m}. The second cube is surrounded by a vacuum. This configuration was chosen because of its geometrical simplicity and because it contains homogeneous subdomains with sharp edges. These edges are known to be a source of numerical difficulties and their presence in the configuration offers an opportunity to investigate how well our method deals with them.

This problem was solved under the condition that edge expansion functions are used when the relative contrast in the numerical value of ε and/or σ in two adjacent tetrahedra exceeds 10%; nodal expansion functions are used in regions with lower contrasts. With this choice edge elements are used along the surfaces of the two cubes; nodal elements are used elsewhere.

The electric field strength of the time-harmonic incident plane wave, having a frequency $f = 10^8$ Hz, can be written as

$$\boldsymbol{E}^{\text{inc}} = \cos(\omega(t - x_3/c_0))\boldsymbol{i}_1, \tag{10}$$

where $\omega = 2\pi f$ denotes the angular frequency and where $c_0 = \omega(\varepsilon_0\mu_0)^{-1/2}$ denotes the speed of light *in vacuo*.

Using symmetry, the domain of computation, $\mathcal{D}_3$, is chosen as $\mathcal{D}_3$ {0 $\leq x_1 \leq$ 0.225 m, 0 $\leq x_2 \leq$ 0.225 m, -0.225 $\leq x_3 \leq$ 0.225 m}. The mesh consists of 15×15×30 cubes of equal size, each subdivided into six tetrahedra. For the discretization in time we have chosen a time step $\Delta t = T/20 = 5 * 10^{-10}$ s.

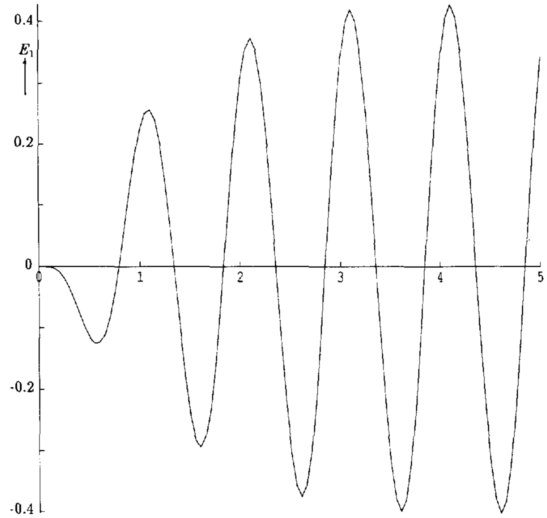

Fig. 1. Transient to time-harmonic, $E_1(x_1 = 0.1, x_2 = 0.1, x_3 = 0, t)$, $0 \leq t \leq 5 * 10^{-8}$s.

The boundary conditions have been chosen as follows: at the plane $x_1 = 0$ the tangential part of electric field strength is set to zero, at the plane $x_2 = 0$ the tangential part of the magnetic field strength is set to zero, and at the the remaining parts of the outer boundary an inhomogeneous absorbing boundary condition is used that exactly absorbs scattered waves that have a normal incidence upon the outer boundary. The initial values at $t = -\Delta t$ and $t = 0$ (a two-step method is used) are set to zero. The transient time is chosen as $t_{\text{tr}} = 5T$, and with this choice an acceptable approximation of the steady state was achieved immediately after the transient period. The medium properties and the frequency chosen are typical for hyperthemia applications. With the discretization used we have a total number of 32 252 degrees of freedom, 1232 of these being set to zero because of the boundary conditions.

In Fig. 1 a plot is given of the transient process. It clearly shows the rapid and smooth transient from zero state to a time-harmonic solution. At $t = t_{\text{tr}}$ the solution has converged to a time-harmonic one to within less than 0.1%; i.e., the time-harmonic solution that can be obtained from the solution immediately after $t = t_{\text{tr}}$ differs less than 0.1% from the time-harmonic solution obtained from results for larger t, when all transients have decayed away. Because of its simple cubic geometry, the realistic choice of contrasts in the medium properties and the difficulty that the interfaces between the different media contain sharp edges, this configuration can serve as a benchmark problem [17] for hyperthermia.

In Fig. 2 a contour plot is given of the real part, $\Re(\hat{E}_1)$, of the complex-valued time-harmonic solution $\hat{E}_1$ in the plane $x_3 = 0$. Note that the real part of the (normal) x component of the electric field strength shows a discontinuity at the outer boundary of the outer cube, reflecting the continuity of the normal flux at that plane. The imaginary part shows the same

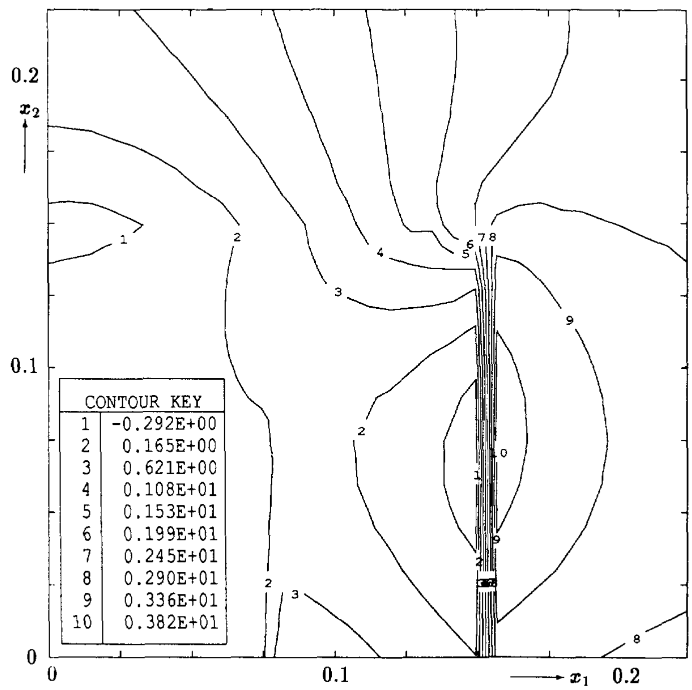

Fig. 2. Contour plot of $\Re(\hat{E}_1(x_1, x_2, x_3 = 0))$.

behavior. Without using (5), the normal components of the electric field strength do not show the proper discontinuity, the errors being larger near the edges of the cubes.

All computations have been carried out at a VAXstation 3100 M76, requiring an average of 2 min of CPU time for each step in time and about 12Mbytes for storing the matrices. The SEPRAN finite-element package [18] is used for carrying out a number of tasks, among them generating the mesh and assembling the system matrices from the element matrices generated by FEMAXT.

VII. Conclusion

The theory discussed in the present paper was implemented in the FEMAXT code that, apart from the time-dependent aspects of it, was developed along the same lines as its counterpart for time-harmonic problems, the FEMAX3 package [19]. We have shown that our approach yields an efficient and very accurate method for computing transient electromagnetic fields in strongly inhomogeneous media. The present time-domain formulation can also be used for the efficient and accurate solution in the time-domain of problems involving time-harmonic fields and as such it is a very attractive alternative to a formulation in the frequency domain.

References

[1] M. Koshiba, K. Hayata and M.Suzuki, "Finite-element formulation of the electric-field vector for electromagnetic waveguide problems," *IEEE Trans. Microwave Theory Tech.*, vol. 33, pp. 900-905, Nov. 1985.

[2] D. R. Lynch and K. D. Paulsen, "Time-domain integration of the Maxwell equations on finite elements," *IEEE Trans. Antennas Propagat.*, vol. 38, pp. 1933-1942, Dec. 1990.

[3] O. B'iró and K. Preis, "Finite element analysis of 3-D eddy currents," *IEEE Trans. Magn.*, vol. 26, pp. 418-423, Mar. 1990.

[4] W. E. Boyse *et al.*, "Nodal-based finite-element modeling of Maxwell's equations," *IEEE Trans. Antennas Propagat.*, vol. 40, pp. 642-651, June 1992.

[5] G. Mur and A. T. de Hoop, "A finite-element method for computing three-dimensional electromagnetic fields in inhomogeneous media," *IEEE Trans. Magn.*, vol. 21, pp. 2188-2191, Nov. 1985.

[6] G. Mur, "Optimum choice of finite elements for computing three-dimensional electromagnetic fields in inhomogeneous media," *IEEE Trans. Magn.*, vol. 24, pp. 330-333, Jan. 1988.

[7] G. Mur, "The finite-element modeling of three-dimensional time-harmonic electromagnetic fields in anisotropic and strongly inhomogeneous media," in *Proc. Int. Symp. and TEAM Workshop* (Okayama, Japan), 11-13 Sept. 1990, pp. 83-86.

[8] G. Mur, "Finite-element modeling of three-dimensional time harmonic electromagnetic fields in inhomogeneous media," *Radio Sci.*, vol. 26, no. 1, pp. 275-280, Jan.-Feb. 1991.

[9] G. Mur, "A mixed finite element method for computing three-dimensional electromagnetic fields in strongly inhomogeneous media," *IEEE Trans. Magn.*, vol. 26, pp. 674-677, Mar. 1990.

[10] G. Mur, "The finite-element modeling of three-dimensional time-domain electromagnetic fields in strongly inhomogeneous media," *IEEE Trans. Magn.*, vol. 28, pp. 1130-1133, Mar. 1992.

[11] J. C. Nédélec, "Mixed finite elements in R3," *Numer. Math.*, vol. 35, pp. 315-341, 1980.

[12] F. Rioux-Damidau *et al.*, "Finite element modeling of electromagnetic fields using different types of variables and boundary conditions," *IEEE Trans. Magn.*, vol. 28, pp. 1126-1129, Sept. 1990.

[13] O. C. Zienkewicz, W. L. Wood, N. W. Hine, and R. L. Taylor, "A unified set of single step algorithms, Part 1: General formulation and application," *Int. J. Numer. Methods Eng.*, vol. 20, pp. 1529-1552, 1984.

[14] O. C. Zienkewicz, "Finite elements in the time domain," ch. 13 in *State of the Art Surveys on Finite-Element Technology*, A. K. Noor and W. D. Pilkey, Eds. American Society of Mechanical Engineers, Applied Mechanics Division, 1983, pp. 405–449.

[15] J. A. Meijerink and H. A. van der Vorst, "Guidelines for the use of

incomplete decompositions in solving sets of linear systems as they occur in practical problems," *J. Comput. Phys.*, vol. 44, pp. 131–155, 1981.

[16] G. Mur, "Absorbing boundary conditions for the finite-difference approximation of the time-domain electromagnetic-field equations," *IEEE Trans. Electromagn. Compat.*, vol. 23, pp. 377-382, Nov. 1981.

[17] A. P. M. Zwamborn, "Scattering by objects with electric contrast," Ph.D. thesis, Delft University, Delft, The Netherlands, 1991.

[18] A. Segal, *SEPRAN, Sepra Analysis, User Manual*, Sepra, Leidschendam, The Netherlands, 1984.

[19] G. Mur, "The FEMAX finite-element package for computing three-Dimensional electromagnetic fields in inhomogeneous media," in *Proc. First Int. Conf. Elec. Eng. Analysis and Design*, 21-23 Aug. 1990, pp. 83–94.

Gerrit Mur received the degree in electrical engineering from the Polytechnic School in Utrecht in 1963. He then received the B.Sc. degree in electrical engineering in 1968, the M.Sc. degree in electrical engineering in 1970, and the Ph.D. degree in technical sciences in 1978, all from the Delft University of Technology.

From 1968-1970 he was a research student with the Laboratory of Electromagnetic Research, Faculty of Electrical Engineering, Delft University of Technology. Since 1970, he has been a member of the Scientific Staff of this laboratory, and is currently an Associate Professor. During the academic year 1979-1980 he held a twelve-month fellowship in the European Science Exchange Program in the Department of Electrical and Electronic Engineering at the University of Nottingham, England. His main research interests are the development of numerical methods for computing electromagnetic fields in inhomogeneous media and/or complicated configurations.